Materials Today Communications 36 (2023) 106875

Contents lists available at ScienceDirect

Materials Today Communications

journal homepage: www.elsevier.com/locate/mtcomm

Ab initio study: Investigating the adsorption behaviors of polarized greenhouse gas molecules on pillar[5]arenes

Quoc Duy Ho *, Eva Rauls

Department of Mathematics and Physics, Universitetet i Stavanger, Norway

ARTICLE INFO

Keywords:
Ab-initio calculations
Adsorption
Nanostructures
Pi interactions
Supramolecular chemistry

ABSTRACT

Supramolecular organic frameworks (SOFs) based on Pillar[5]arenes (P[5]A) have shown great potential in capturing and separating greenhouse gases. In this study, we investigate the adsorption behaviors of other environmentally harmful gas molecules, including NO, NH_3, CO, and NO_2 on pillar[5]arenes (P[5]A) using DFTB and DFT calculations. The P[5]A structures exhibit the capability to adsorb including NO, NH_3, CO, and NO_2 at both the cavity site and OH group, facilitated by π-π interactions and hydrogen bonding. CO exhibits the lowest binding energy among the studied gases, primarily due to its weak dipole moment. In contrast, the cavity-in positions for NO_2 and NH_3, characterized by high polarization, exhibit the highest adsorption energies. The adsorption energies at the top-out positions are relatively similar for all gases examined. These findings provide valuable insights for the targeted design and optimization of P[5]A, enabling its potential applications in effectively capturing toxic gases.

1. Introduction

Global warming, a significant component of climate change, is primarily caused by the elevated concentrations of greenhouse gases resulting from human activities. While carbon dioxide (CO_2) remains the primary contributor to the greenhouse effect, other polarized-contributed greenhouse gases, such as carbon monoxide (CO), nitrogen oxide (NO), ammonia (NH_3), and nitrogen dioxide (NO_2), have also gained considerable attention. In recent years, numerous studies have focused on reducing the emissions of greenhouse gases, and adsorption has emerged as an efficient method for their capture. Various materials, including metal oxides, zeolites, metal-organic frameworks (MOFs), and supramolecular organic frameworks (SOFs), have been investigated for this purpose [1–11]. One of the most promising contenders among them is the supramolecular organic framework known as pillar[*n*]arenes (P[*n*]A). This framework exhibits exceptional potential due to its straightforward synthesis, easy chemical handling, remarkable chemical and thermal stability, water solubility, and, notably, its outstanding host-guest properties [9,12–14].

Since the synthesis of P[5]A by Ogoshi et al.[15] in 2008, this material has gained significant attention for its potential in CO_2 capture applications. Experimental and theoretical studies [9,16,17] have demonstrated the advantages of using P[*n*]A for CO_2 adsorption. In our previous research on CO_2 adsorption using P[*n*]A [16,17], we observed that this material can adsorb CO_2 molecules at both the cage cavity site and the hydroxyl group, facilitated by π-π and hydrogen bonding interactions, respectively. This multi-site interaction capability enhances the effectiveness of P[*n*]A for CO_2 capture compared to other materials. Additionally, the physisorption nature of CO_2 by P[*n*]A allows for the possibility of desorbing and reusing the material after an appropriate CO_2 desorption process. Furthermore, due to the weak interaction between CO_2 molecules, additional CO_2 molecules can be accommodated within the complex even after the cavity site is filled.

In this paper, our objective is to show that beside the physical adsorption of CO_2, P[5]A can also adsorb other greenhouse polarized gases such as including NO, NH_3, CO, and NO_2. We will discuss the fundamental principles governing the adsorption process, focusing on the interactions between the polarized gases and P[5]A, utilizing a DFT-based method. By analyzing and presenting the results of our research, we aim to contribute to the understanding of the adsorption behavior and potential applications of P[5]A in the field of greenhouse gases capture.

2. Computational details

The calculations performed in our study employed the self-consistent

* Corresponding author.
E-mail address: duy.hoquoc@uis.no (Q.D. Ho).

https://doi.org/10.1016/j.mtcomm.2023.106875
Received 8 July 2023; Received in revised form 9 August 2023; Accepted 11 August 2023
Available online 17 August 2023

charge density-functional-based tight-binding (SCC-DFTB) method [18–20] implemented in the DFTB+ 22.1 code [21]. These DFTB calculations demonstrate a high level of agreement with density functional theory (DFT) results, while significantly reducing computational costs [22]. This agreement has been previously confirmed in our investigation of the pillar[5]arenes system [16,17]. Furthermore, an advantage of the DFTB method is that, despite employing localized basis sets, it is not subject to the significant basis set superposition error [23]. In our calculations, we utilized the *mio-1–1* basis set [19] with the electron core held frozen. Carbon, oxygen, and nitrogen atoms utilized *2 s* and *2p* valence orbitals, hydrogen atoms employed *1 s* orbitals. To account for van der Waals interactions, the *SimpleDftD3* dispersion correction scheme was implemented. The structural calculations included a vacuum space of at least 15 Å to prevent periodic image interactions. A convergence condition of 10^{-4} eV was applied to the self-consistent electronic energy, and during the relaxation calculation, optimization was halted when the maximum forces dropped below 10^{-4} eV/A. Finally, the Γ *k*-point approximation [24] was utilized throughout all calculations, while a higher *k*-point sampling of 4×4x4 was employed for the density of states (DOS) calculation. Convergence was verified using a *k*-point mesh of 6×6x6. To examine the charge transfer from P[5]A to the gas molecules, we utilized the Bader charge transfer method [25] with VASP 5.4.4 and the projector augmented wave method [26–28]. The plane-wave basis set was truncated at 400 eV, and the exchange effects were modeled using PBE.

3. Results and discussion

The adsorption energy of polarized gases on P[5]A has been calculated using the following equation:

$$E_{ads} = E_{P[5]A+gas} - \left(E_{P[5]A} + E_{gas}\right)$$

Here, E_{ads} represents the adsorption energy $E_{P[5]A+\mathrm{gas}}$ is the total energy of P[5]A with the adsorbed gas $E_{P[5]As}$ is the total energy of P[5]A, and E_{gas} is the isolated gas molecule energy. A higher negative value indicates a more favorable adsorption, indicating a stronger attraction of energy between P[5]A and the adsorbed gas.

It is important to mention that in weak interaction systems, the correction for zero-point energy (ZPE) can have a significant impact. The influence of ZPE on adsorption energy has been extensively studied by Govender et al.[29]. According to their research, the ZPE correction derived from C-H bonds can exert a notable impact, ranging from 0.2 to 0.3 eV. However, Govender and colleagues [29] also argued that when it comes to physical adsorption, the inclusion of ZPE correction merely brings about a negligible change in the adsorption energy. In our current investigation, we observed that no new C-H bonds were formed during the adsorption process, and the gases were physisorbed by P[5]A. Hence, considering the ZPE is not anticipated to yield substantial discrepancies in our findings. In our previous study, we reaffirmed the point by demonstrating that the inclusion of ZPE correction has minimal effect on the adsorption energy of CO_2 at P[5]A [17].

3.1. CO adsorption

Fig. 1 below depicts the adsorption behavior of carbon monoxide (CO) on P[5]A. The adsorption behavior of CO on P[5]A differs slightly from that of CO_2 [16]. CO shows adsorption only at the cavity-in and top-out positions of P[5]A, with no observed adsorption at the top-in configuration. When the CO molecule is initially positioned at the top-in location, it eventually transitions to the cavity-in position (Fig. 1a). This phenomenon arises from the weaker interaction between CO and the OH group compared to the attraction between CO and the π electron of P[5]A, leading the CO molecule to be pulled towards the cavity-in position. Given that oxygen (O) possesses a higher electronegativity (3.44) in comparison to carbon (C) (2.55), it is expected that in the top-out adsorbed position, the CO molecule would align towards the OH group, with the oxygen atom of CO closer to the hydrogen (H) atom of OH. Similar to the scenario involving CO2 adsorption in the top-in and top-out configurations, the oxygen atom of CO_2 forms a hydrogen bond with the hydroxyl (OH) group of P[5]A [16]. However, our calculations revealed that in the top-out configuration, the C is closer to the OH group. These calculated findings align with the observations made by Kim and colleagues [30] who characterized CO as a quadrupole-driven molecule with a very weak dipole moment. In their study, both ends of the CO molecule, C and O, exhibited negative electrostatic potential (EP), with the C end displaying a more negative EP than the O end [30]. Table 1 provides the adsorption energies of CO, showcasing that the binding energy at the cavity site surpasses that at the OH functional group, primarily due to the stronger π-π interaction at the cavity site compared to the hydrogen bonding at the functional group.

When comparing with the earlier findings regarding CO_2 adsorption onto P[5]A [16], notable distinctions emerge. Besides the variance in

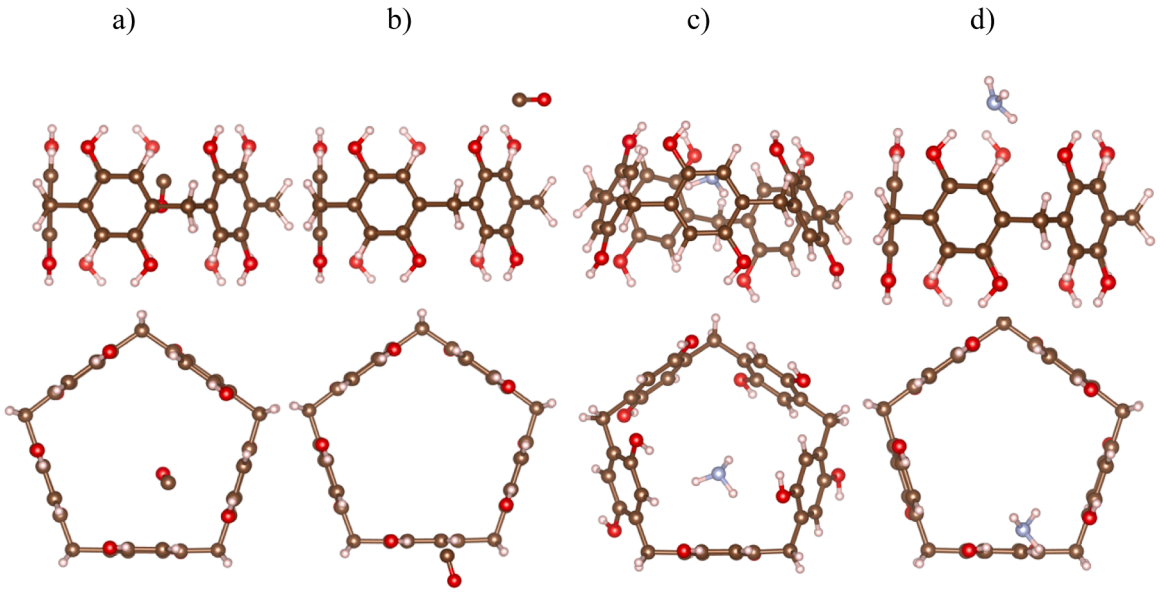

Fig. 1. Atomic structures of adsorbed a) CO cavity-in, b) CO top, c) NH_3 cavity-in, and d) NH_3 top from side view and top view.

Table 1
CO, NO, and NO_2 adsorption energies in (eV) in the three different positions. the results obtained with the DFTB-code.

Position	CO	NH_3	NO	NO_2
Cavity-in	-0.27	-0.49	-0.31	-0.45
Top-in	n/a	-0.27	-0.17	-0.28
Top-out	-0.12	n/a	-0.16	-0.13

the count of adsorption sites on P[5]A – 2 versus 3 adsorption sites – the binding energy of CO exhibits a reduction in comparison to CO_2. Specifically, CO manifests lower binding energies (−0.35 eV and −0.17 eV for the cavity-in and top-out configurations, respectively) attributed to its notably feeble dipole moment.

Table 2 above illustrates the transfer of charge between P[5]A and polarized gases. The table distinctly reveals that due to their weaker dipole moments, gases like CO and NH_3 acquire a notably lower quantity of electrons from P[5]A compared to the significant electron uptake observed from P[5]A by NO and NO_2, particularly in the context of the cavity-in configuration involving π-π interactions.

3.2. NH_3 adsorption

Table 1 also provides the binding energies of NH_3 with P[5]A. Despite NH_3 being an uncharged molecule, it exhibits an asymmetric charge distribution, with positively charged hydrogen nuclei surrounding a central nitrogen atom. This unique charge arrangement imparts NH_3 with a relatively polar nature. Upon interacting with P[5]A, NH_3 can be adsorbed either at the OH group or at the cavity site. The interaction between NH_3 and the OH group is weaker in comparison to the interaction with the cavity site. As a result, when NH_3 is shifted towards the cavity site, it also assumes the cavity-in configuration like CO and CO_2 gases, as illustrated in Fig. 1c. The observed preference for the cavity-in position is further supported by the adsorption energy values presented in Table 1. The binding energy of NH_3 in the cavity-in configuration is significantly higher compared to NH_3 adsorbed at the OH group. In the cavity-in configuration, NH_3 engages in two types of interactions with P[5]A. The positively charged hydrogen atoms are attracted to the benzene rings, while the negatively polarized nitrogen atom interacts with the hydrogen atoms of the OH groups. These interactions lead to a closer rotation of the arenes in P[5]A towards the NH_3 molecule. The interaction between NH_3 and P[5]A diverges from the interactions observed between CO and CO_2 with P[5]A, where π-π interactions assume a prominent role. Furthermore, the charge transfer calculation confirms the positive behavior of H and negative behavior of nitrogen (N) in the interaction between NH_3 and P[5]A. Specifically, NH_3's adsorption at the cavity site involves gaining electrons from P[5]A through the interaction between the positive H of NH_3 and the π electron of the benzene rings, while in the top position, N of NH_3 provides electrons to the OH group.

3.3. NO and NO_2 adsorption

Fig. 2 illustrates the adsorption of NO gas on P[5]A, showcasing distinct interaction behaviors compared to CO. The polar nature of NO arises from the higher electronegativity of oxygen (3.44) in comparison to nitrogen (3.04), resulting in greater electron density at O atom than at N [16]atom. Consequently, the N atom of NO is positioned closer to the benzene ring of P[5]A, while the O atom of NO points towards the H atom of the OH groups. P[5]A can adsorb NO at three different positions: cavity-in, top-in, and top-out as shown in Fig. 2. Among these positions, the cavity-in site exhibits the highest binding energy. The adsorbed NO at the cavity-in configuration (Fig. 2a) demonstrates the most favorable adsorption energy (−0.31 eV). When NO comes into contact with the benzene rings of P[5]A, it undergoes adsorption onto the benzene rings through a π-π interaction. This interaction takes place between the π electrons of the benzene ring and the antibonding π * orbital of NO. The π electrons of the benzene ring align with the nodal plane of the π * orbital of NO, resulting in a favorable overlap and stabilization. The adsorption energies of NO for the top-in and top-out configurations are relatively similar (−0.17 eV vs −0.16 eV), even though interaction behaviors are quite different. In the top-out configuration, NO is attracted to P[5]A through hydrogen bonding with the OH group. On the other hand, in the top-in configuration, the N atom of NO is attracted to the π electron of the benzene ring, while the O atom interacts with the nearest OH group. The primary force driving the top-out configuration of NO is hydrogen bonding, resulting in a nearly zero charge transfer between P[5]A and NO (Table 2). However, in the presence of π-π interaction, the charge transfer is higher, with the highest charge transfer observed for the cavity-in configuration of NO that shows the Lewis acid-like behavior of adsorbed NO-cavity-in in the interaction with P[5]A. It is worth noting that due to polarization effects, the charge transfer in NO is higher compared to weakly dipolar CO and non-polar CO_2 [16].

In comparison to NO, NO_2 exhibits stronger polarization, leading to a greater charge transfer between P[5]A and NO_2 when π electrons are involved in the interaction. Fig. 3 illustrates the adsorbed positions of NO_2 on P[5]A, including cavity-in, top-in, and top-out configurations. The Lewis structure of NO_2 consists of a central nitrogen atom bonded to two oxygen atoms. The nitrogen atom possesses a lone pair of electrons, while each oxygen atom has two lone pairs. The lone pair of electrons on nitrogen pushes the two oxygen atoms to one side of the molecule, resulting in a bond angle of approximately 130 degrees. This asymmetry polarizes NO_2, generating a partial negative charge (δ-) on the oxygen atom and a partial positive charge (δ +) on the nitrogen atom. The polarization of NO_2 causes the nitrogen atom to exhibit a partial positive charge, directing it towards the benzene ring of P[5]A in the cavity-in configuration. Consequently, more electrons are transferred between NO_2 and P[5]A compared to the transfer from P[5]A to CO_2 [16]. As a result, the adsorption energy of NO_2 in the cavity-in and top-in configurations is higher than that of CO_2.

Table 2
Amount of charge transferred [e] from P[5]A to the gas molecules in the three positions.

Position	CO	NH_3	NO	NO_2
Cavity-in	0.063	0.022	0.176	0.233
Top-in	n/a	-0.045	0.097	0.119
Top-out	-0.006	n/a	0.010	0.009

3.4. Density of states (DOS)

When using a material for gas adsorption applications, the ability to reuse the material through a desorption procedure is of utmost importance. In our previous study we demonstrated the reusability of P[5]A for CO_2 adsorption [16]. In this study, our aim is to showcase that P[5]A can also be effectively utilized and reused for the adsorption of polarized greenhouse gases. To assess any potential changes, we calculated and plotted the density of states (DOS) of P[5]A before and after gas adsorption, as depicted in the Fig. 4. The adsorption of gases onto P[5]A occurs either at the cavity site or on the surface, primarily driven by weak interactions such as van der Waals forces and hydrogen bonds. No chemical bonding was observed during the adsorption process, indicating that there is no significant alteration in the DOS of P[5]A before and after gas adsorption. Among the cases studied, the adsorbed NO_2 and NH_3 in the cavity-in configuration exhibited the highest adsorption energy and charge transfer from P[5]A, respectively. Therefore, we chose the P[5]A sample after NO_2 and NH_3 adsorption to plot the DOS.

The plotted figure illustrates the DOS of P[5]A before and after adsorption. Remarkably, the DOS remains largely undisturbed after adsorption. This calculated outcome suggests that the structure of P[5]A remains unchanged following adsorption, implying that the adsorption

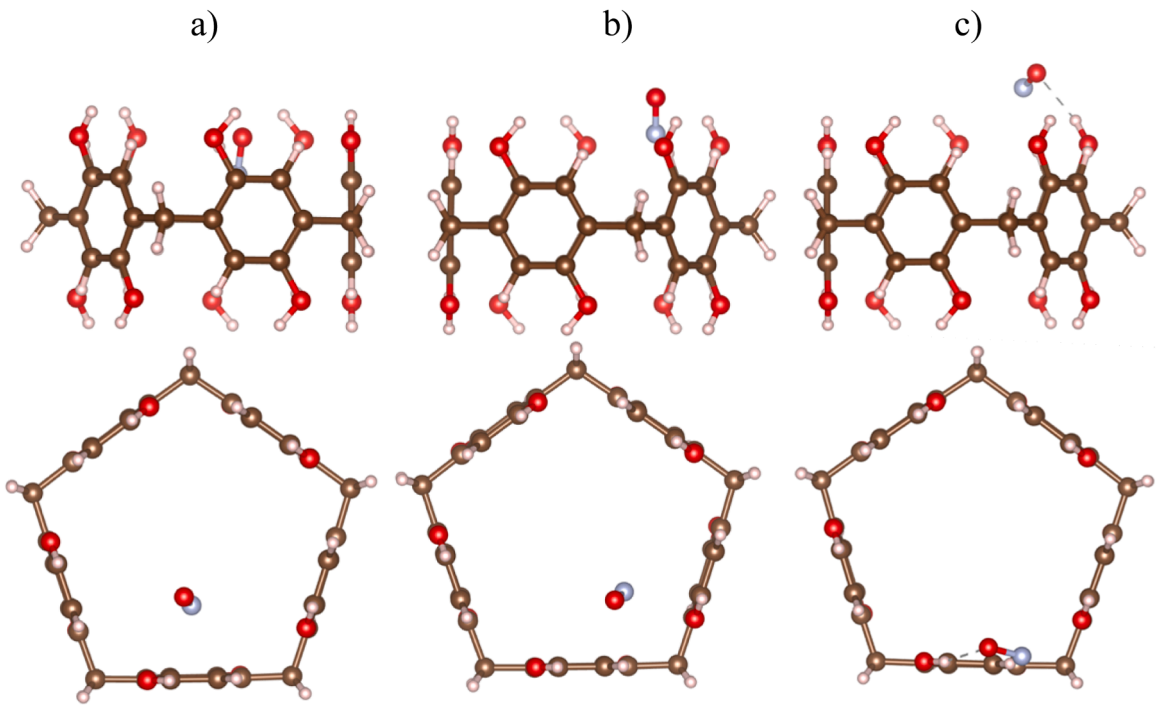

Fig. 2. Atomic structures of NO gas adsorption at P[5]A at a) cavity-in, b)top-in, and c) top-out from side view and top view.

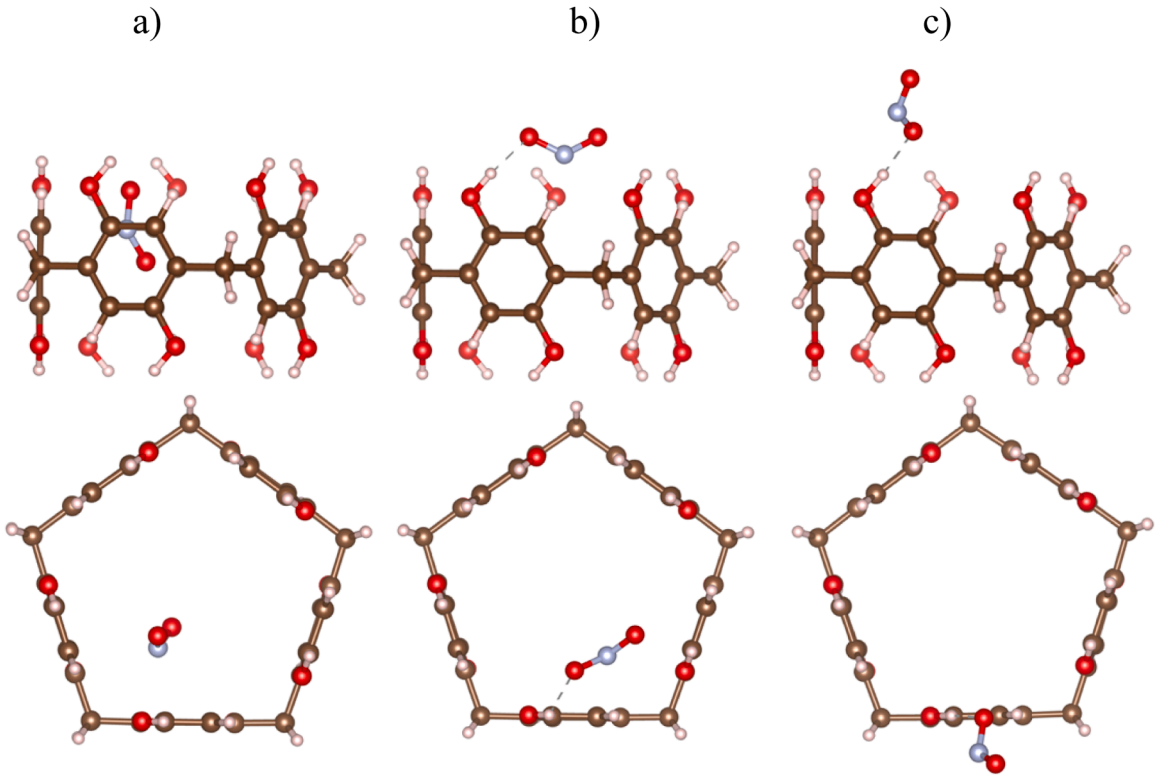

Fig. 3. Atomic structures of NO_2 gas adsorption at P[5]A at a) cavity-in, b)top-in, and c) top-out from side view and top view.

of NO_2 and NH_3 does not cause any noticeable erosion or degradation of P[5]A. Overall, our findings indicate that P[5]A exhibits promising reusability for gas adsorption purposes, including the capture of polarized greenhouse gases. The preservation of P[5]A's structural integrity further supports its potential for sustainable and efficient gas adsorption applications.

4. Conclusion

The adsorption behavior of CO, NH_3, NO, and NO_2 gases on P[5]A was investigated using density functional theory (DFT)-based calculation methods. Similar to CO_2 adsorption, both weak hydrogen bonds and π-π interactions contribute to the stabilization of the adsorbates on P[5]

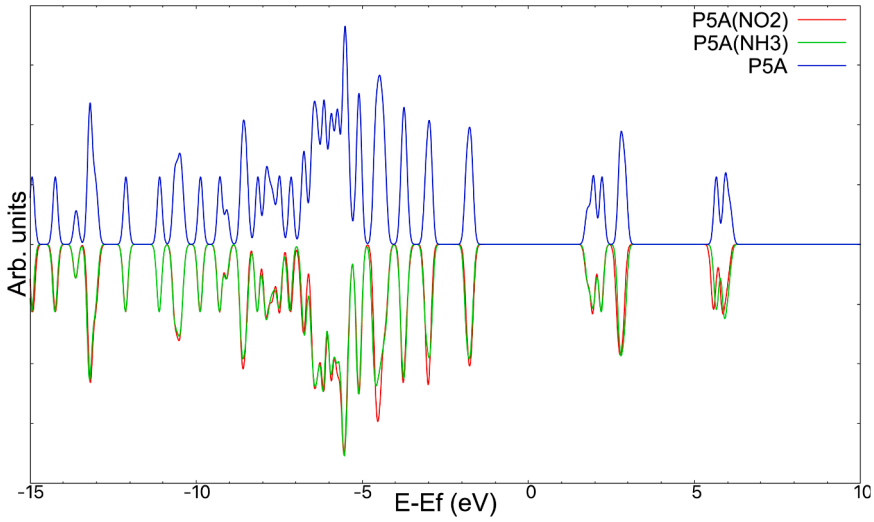

Fig. 4. DOS of pure P[5]A (blue), P[5]A after NO_2 (red) and NH_3 (green) adsorption at cavity-in positions.

A. Specifically, in the cavity site, the π-π interaction between the benzene rings of the arenes and the adsorbate plays a crucial role. The polarized gases, particularly NO and NO_2, exhibit an acid-like behavior, where P[5]A acts as a Lewis base in the acid-base interaction scheme. Hydrogen bonding predominantly occurs at the OH group. The binding energy of CO is the lowest among the studied gases, attributed to its very weak dipole moment. Conversely, due to their high polarization, the cavity-in positions of NO_2 and NH_3 display the highest adsorption energies, while the adsorption energies at the OH functional groups are relatively similar. Calculation results demonstrate that the DOS of P[5]A shows no significant changes when adsorbing the gases, indicating that P[5]A can be effectively reused for subsequent adsorption procedures.

CRediT authorship contribution statement

Quoc Duy Ho: Conceptualization, Methodology, Software, Data curation, Writing – original draft preparation. **Eva Rauls**: Investigation, Supervision, Writing – review & editing.

Declaration of Competing Interest

The authors declare that they have no known competing financial interests or personal relationships that could have appeared to influence the work reported in this paper.

Data Availability

Data will be made available on request.

Acknowledgments

The authors greatly acknowledge financial support of the Research Council of Norway within project 324306 in the PETROMAKS 2 program. The calculations with VASP performed on resources provided by Sigma2 - the National Infrastructure for High Performance Computing and Data Storage in Norway (project NN8071K).

References

[1] B. Feng, H. An, E. Tan, Energy Fuels 21 (426) (2007).
[2] Q.-L. Tang, Q.-H. Luo, J. Phys. Chem. C. 117 (2013) 22954.
[3] G.A. Mutch, S. Shulda, A.J. McCue, M.J. Menart, C.V. Ciobanu, C. Ngo, J. A. Anderson, R.M. Richards, D. Vega-Maza, J. Am. Chem. Soc. 140 (2018) 4736.
[4] W. Jeong, J. Kim, J. Phys. Chem. C. 120 (2016) 23500.
[5] J.G. Min, K.C. Kemp, H. Lee, S.B. Hong, J. Phys. Chem. C. 122 (2018) 28815.
[6] J.-R. Li, Y. Ma, M.C. McCarthy, J. Sculley, J. Yu, H.-K. Jeong, P.B. Balbuena, H.-C. Zhou, Coord. Chem. Rev. 255 (2011) 1791.
[7] J. Yu, L.-H. Xie, J.-R. Li, Y. Ma, J.M. Seminario, P.B. Balbuena, Chem. Rev. 117 (2017) 9674.
[8] Q. Wang, D. Astruc, Chem. Rev. 120 (2020) 1438.
[9] L.-L. Tan, H. Li, Y. Tao, S.X.-A. Zhang, B. Wang, Y.-W. Yang, Adv. Mater. 26 (2014) 7027.
[10] J. Lü, et al., J. Am. Chem. Soc. 136 (2014) 12828.
[11] R.S. Patil, D. Banerjee, C. Zhang, P.K. Thallapally, J.L. Atwood, Angew. Chem. Int. Ed. 55 (2016) 4523.
[12] C. Li, Q. Xu, J. Li, Y. Feina, X. Jia, Org. Biomol. Chem. 8 (1568) (2010).
[13] T. Ogoshi, R. Shiga, T.-a Yamagishi, Y. Nakamoto, J. Org. Chem. 76 (2011) 618.
[14] C. Li, L. Zhao, J. Li, X. Ding, S. Chen, Q. Zhang, Y. Yu, X. Jia, Chem. Commun. 46 (2010) 9016.
[15] T. Ogoshi, S. Kanai, S. Fujinami, T.-a Yamagishi, Y. Nakamoto, J. Am. Chem. Soc. 130 (2008) 5022.
[16] Q. Duy Ho, E. Rauls, e202204215, ChemistrySelect 8 (2023). e202204215.
[17] Q. Duy Ho, E. Rauls, e202302266, ChemistrySelect 8 (2023). e202302266.
[18] D. Porezag, T. Frauenheim, T. Köhler, G. Seifert, R. Kaschner, Phys. Rev. B 51 (1995) 12947.
[19] M. Elstner, D. Porezag, G. Jungnickel, J. Elsner, M. Haugk, T. Frauenheim, S. Suhai, G. Seifert, Phys. Rev. B 58 (1998) 7260.
[20] G. Seifert, J. Phys. Chem. A 111 (2007) 5609.
[21] B. Aradi, B. Hourahine, T. Frauenheim, J. Phys. Chem. A 111 (2007) 5678.
[22] T. M. F. Elstner, J. McKelvey, G. Siefert, J. Phys. Chem. A 111 (2007) 5607.
[23] R. Luschtinetz, J. Frenzel, T. Milek, G. Seifert, J. Phys. Chem. C. 113 (2009) 5730.
[24] H.J. Monkhorst, J.D. Pack, Phys. Rev. B 13 (1976) 5188.
[25] W. Tang, E. Sanville, G. Henkelman, J. Phys.: Condens. Matter 21 (2009), 084204.
[26] G. Kresse, J. Hafner, Phys. Rev. B 49 (1994) 14251.
[27] G. Kresse, J. Furthmüller, Phys. Rev. B 54 (1996) 11169.
[28] G. Kresse, D. Joubert, Phys. Rev. B 59 (1999) 1758.
[29] A. Govender, D. Curulla Ferré, J.W. Niemantsverdriet, ChemPhysChem 13 (2012) 1591.
[30] H. Kim, V.D. Doan, W.J. Cho, R. Valero, Z. Aliakbar Tehrani, J.M.L. Madridejos, K. S. Kim, Sci. Rep. 5 (2015), 16307.